Biochemical and Biophysical Research Communications 527 (2020) 226–231

Contents lists available at ScienceDirect

Biochemical and Biophysical Research Communications

journal homepage: www.elsevier.com/locate/ybbrc

Crystal structure of PD-1 in complex with an antibody-drug tislelizumab used in tumor immune checkpoint therapy

Sang Hyung Lee [1], Hyun Tae Lee [1], Heejin Lim [1], Yujin Kim, Ui Beom Park, Yong-Seok Heo*

Department of Chemistry, Konkuk University, 120 Neungdong-ro, Gwangjin-gu, Seoul, 05029, Republic of Korea

ARTICLE INFO

Article history:
Received 21 April 2020
Accepted 23 April 2020

Keywords:
PD-1
Tislelizumab
Antibody
Crystal structure
Immune checkpoint
Cancer immunotherapy

ABSTRACT

Blocking of the interaction between Programmed cell death 1 (PD-1) and its ligand PD-L1 by monoclonal antibodies has elicited unprecedented therapeutic benefits and achieved a major breakthrough in immunotherapy of multiple types of tumors. Here, we determined the crystal structure of PD-1 in complex with the Fab fragment of tislelizumab. This monoclonal antibody was approved in December 2019 by the China National Medical Product Administration for Hodgkin's lymphoma and is under multiple clinical trials in China and the US. While the three complementarity determining regions (CDRs) in the light chain are involved in the target interaction, only CDR3 within the heavy chain interacts with PD-1. Tislelizumab binds the front β-sheet of PD-1 in a very similar way as PD-L1 binds to PD-1, thereby blocking the PD-1/PD-L1 interaction with a higher affinity. A comparative analysis of PD-1 interactions with therapeutic antibodies targeting PD-1 provides a better understanding of the blockade mechanism of PD-1/PD-L1 interaction in addition to useful information for the improvement of therapeutic antibodies capable of diminishing checkpoint signaling for cancer immunotherapy.

1. Introduction

Programmed cell death 1 (PD-1) is an immune checkpoint protein on T cells and plays a pivotal role in modulating immune responses [1]. The interaction of PD-1 with its ligands PD-L1 and PD-L2 on antigen-presenting cells induces co-inhibitory signals attenuating T-cell activity [2,3]. PD-L1 and PD-L2 are highly expressed in tumor cells, enabling the tumor cells to evade T cell-mediated immune responses. Blockade of the interaction of PD-1 with its ligands PD-L1 and PD-L2 can enhance T-cell activity and prevents tumor cells from avoiding the immune surveillance [4,5].

Monoclonal antibodies targeting immune checkpoint proteins, including PD-1, PD-L1, and CTLA-4, have elicited significant therapeutic benefits in cancer patients and provided a breakthrough in the field of immune-oncology [6,7]. While targeted therapies of cancer usually demonstrate transient clinical responses due to the acquisition of drug resistance within several months after administration, the clinical responses of the monoclonal antibodies against checkpoint proteins are often durable, without inducing cancer progression for many years [8]. To date, three antibody drugs targeting PD-1 have been approved by the US FDA. These antibody drugs block the interaction of PD-1 with its ligands, thereby reversing the PD-1 pathway-mediated immunosuppression. Two of these antibodies, nivolumab and pembrolizumab, were approved by the US FDA in 2014 for the treatment of melanoma, non-small cell lung cancer, and multiple types of cancers [9,10]. In 2018, the US FDA approved the third anti-PD-1 antibody, cemiplimab, for treating patients with metastatic cutaneous squamous cell carcinoma and locally advanced cutaneous squamous cell carcinoma who are not candidates for curative surgery or curative radiation [11].

Tislelizumab, a humanized IgG4 monoclonal antibody against PD-1, was conditionally approved in China in December 2019 for the treatment of relapsed or refractory classical Hodgkin's lymphoma after at least second-line chemotherapy, and full approval will be granted based on confirmatory randomized clinical trials [12]. It is designed to bind less to Fc-γ receptor 1 (FcγRI) to enhance the anti-cancer efficacy of the antibody drug [13]. As a result of the crosslinking between PD-1 expressing effector T cells and FcγRI expressing macrophages, the anti-cancer efficacy of the FDA-approved antibody drugs targeting PD-1, including nivolumab and pembrolizumab, can be attenuated due to antibody-dependent cellular phagocytosis of T cells by macrophages [13].

* Corresponding author.
E-mail address: ysheo@konkuk.ac.kr (Y.-S. Heo).
[1] These authors contributed equally to this work.

https://doi.org/10.1016/j.bbrc.2020.04.121
0006-291X/

In recent years, the crystal structures of the FDA-approved antibody drugs in complex with PD-1 or PD-L1 were determined, providing a structural basis for antibody-based blockade of PD-1 and PD-L1 in cancer immunotherapy [14,15]. The binding characteristics and blocking mechanisms of the two anti-PD-1 antibodies, nivolumab and pembrolizumab, were reported to be quite different [16]. Nivolumab mainly binds to the N-terminal region of PD-1, which is outside the Ig-like domain that contributes to PD-L1 binding, while pembrolizumab mainly binds to the C'D loop, which is also not involved in the PD-L1 binding [17,18]. Although the epitopes of nivolumab and pembrolizumab on the surface of PD-1 are different, the binding of these two antibodies is competitive to each other [18]. However, whether these two antibody drugs are representative of all the binding modes of anti-PD-1 antibodies is unknown. There are more anti-PD-1 antibodies under clinical trials, and investigations of the binding mechanisms of these anti-PD-1 antibodies would provide a better understanding of antibody-based blockade of PD-1 and PD-L1 for immune checkpoint inhibitor therapy.

Here, we determined the crystal structure of PD-1 in complex with the Fab fragment of tislelizumab to elucidate the specific interaction between tislelizumab and PD-1. The dominant binding to the front β-sheet of PD-1 with three CDR loops of its light chain and CDR3 of the heavy chain is substantially different compared to that of nivolumab and pembrolizumab. Our findings not only help to provide a better understanding of the molecular mechanism of tislelizumab but also broadens our knowledge about antibody-based checkpoint blockade.

2. Materials and methods

2.1. Cloning, expression, and purification

The proteins of PD-1 and tislelizumab Fab were prepared as described previously [14]. In brief, the extracellular domain of human PD-1 (aa 26–150) was expressed in *E. coli* as inclusion bodies and recovered by the refolding process using 8 M urea as a denaturing reagent. The refolded protein was purified by the Ni-affinity and gel filtration chromatography. The DNA sequences for the heavy and light chains of the Fab fragment of tislelizumab was codon-optimized, synthesized, and subcloned into a modified pBAD vector. The tislelizumab Fab fragment was obtained by periplasmic expression in *E. coli* and purified by the Ni-affinity and gel filtration chromatography.

2.2. Crystallization of PD-1/tislelizumab Fab complex

The mixture of purified PD-1 and tislelizumab Fab fragment was incubated for 1 h at 4 °C, and the complex of PD-1/tislelizumab Fab was separated by size exclusion chromatography. The purified protein of the PD-1/tislelizumab Fab complex was concentrated to 12 mg mL^{-1} in a buffer containing 20 mM Tris, pH 8.0, and 300 mM NaCl, and crystallized by hanging-drop vapor diffusion method with a well solution containing 0.2 M ammonium sulfate, 30% (w/v) polyethylene glycol 4000 at 20 °C within a week. Before data collection, the crystals were cryocooled using a cryoprotectant consisting of the reservoir solution supplemented with 20% glycerol.

2.3. Data collection and structure determination

The X-ray diffraction data were collected on beamline 5C at Pohang Accelerator Laboratory at the wavelength of 1.00 Å. The diffraction data set was processed and scaled using HKL2000 software package [19]. The structure of the PD-1/tislelizumab Fab complex was determined by molecular replacement with the program Phaser using a structure of Fab that has high sequence homology with tislelizumab (PDB code 4KY1, chains H and L) and PD-1 in the structure of PD-1/pembrolizumab complex (PDB code 5GGS, chains Y) as search models [20]. As the elbow region of an antibody Fab is intrinsically flexible, the variable and constant regions of the search model for Fab were separated during MR phasing. The initial electron density map corresponding to two copies of the PD-1/tislelizumab Fab complex was prominent in an asymmetric unit. Model building and refinement were carried out iteratively using Coot and PHENIX [21,22]. Statistics for data collection and refinement can be found in Table 1. All structural figures were generated using Pymol (http://www.pymol.org). The atomic coordinates and structure factors for the structure of PD-1/tislelizumab complex have been deposited in Protein Data Bank (PDB, http://www.rcsb.org) under the entry 7BXA.

3. Results

3.1. Crystal structure of the PD-1/tislelizumab Fab complex

In this study, the extracellular domain (residues 26–150) of human PD-1 was expressed as inclusion bodies in *E. coli*, and its soluble form was obtained by *in vitro* refolding process. The Fab fragment of tislelizumab was expressed in the periplasmic space of *E. coli*. Size exclusion chromatography confirmed that the 1:1 complex of PD-1 and the tislelizumab Fab exists as a monomer in solution. The complex structure of PD-1 with the tislelizumab Fab was solved and refined to a resolution of 3.32 Å, with $R/R_{free} = 0.243/0.299$. An asymmetric unit in the crystals contained two copies of the complex without any symmetric relationship between them (Fig. 1A). Superposition of the structures of PD-1 from the two copies in an asymmetric unit showed that the bound Fab was tilted slightly, whereas the PD-1 protein and the three CDRs of the light chain and only the CDR3 loop of the heavy chain of tislelizumab exhibited little structural deviation from each other (Fig. 1B). This tilt may be due to the unique characteristics of the interaction of tislelizumab, which is mediated by LCDR1, LCDR2, LCDR3, and HCDR3, leaving HCDR2 and HCDR2 without any binding to PD-1 (Fig. 1D). In the previously reported structure of PD-1 in complex with nivolumab or pembrolizumab, all of the six CDRs of these two antibodies are involved in the interaction with PD-1 [14]. Almost all residues of the two copies in an asymmetric unit, except for a few residues within the flexible loops of PD-1, were clearly visualized in the electron density map, elucidating the precise interactions within the interface between PD-1 and tislelizumab despite the low resolution of the structural data (Fig. 1C).

3.2. Blocking mechanism and molecular interaction of tislelizumab

To explore the blocking mechanism of tislelizumab to the interaction of PD-1/PD-L1, the PD-1 protein of the PD-1/tislelizumab complex was superimposed onto the PD-1/PD-L1 complex (PDB code 3BIK) [23,24]. Overall, the binding of tislelizumab to PD-1 exhibited a stereospecific hindrance to that of PD-L1. Specifically, the variable region of the tislelizumab light chain provides major conflicts with PD-L1, while its heavy chain except HCDR3 is away from the binding interface of PD-1/PD-L1 (Fig. 2A). The interaction between tislelizumab and PD-1 buries a total solvent accessible area of 2014 $Å^2$, which is slightly larger than the binding interface of PD-1/PD-L1 (1970 $Å^2$). Most of the buried solvent accessible area is contributed by the light chain (71%). The extracellular domain PD-1 is an Ig-like domain containing two β-sheets, the front β-sheet consisting of the CC'FG strands and the back β-sheet consisting of the AA'BDE strands. The interaction

Table 1
Data collection and refinement statistics.

Data Collection	
X-ray source	PLS 5C
Wavelength (Å)	1.0000
Space group	$P2_12_12_1$
a, *b*, *c* (Å)	64.61, 73.08, 276.39
Resolution (Å)	3.32 (3.39–3.32)[a]
R_{sym} (%)	17.8 (42.9)
$I/\sigma I$	11.3 (2.0)
Completeness (%)	99.3 (100.0)
Redundancy	4.5 (4.1)
$CC_{1/2}$	0.947 (0.788)
Refinement	
Resolution (Å)	3.32
No. reflections	19790
R_{work}/R_{free} (%)	24.3/29.9
No. atoms	
Protein	8095
Water	0
Average B-factor (Å^2)	35.0
R.m.s. deviation	
Bond lengths (Å)	0.004
Bond angles (°)	1.303
Ramachandran	
Favored (%)	97.08
Allowed (%)	2.92
Outlier (%)	0.00
PDB code	7BXA

[a] Values in parentheses are for the outer resolution shell.

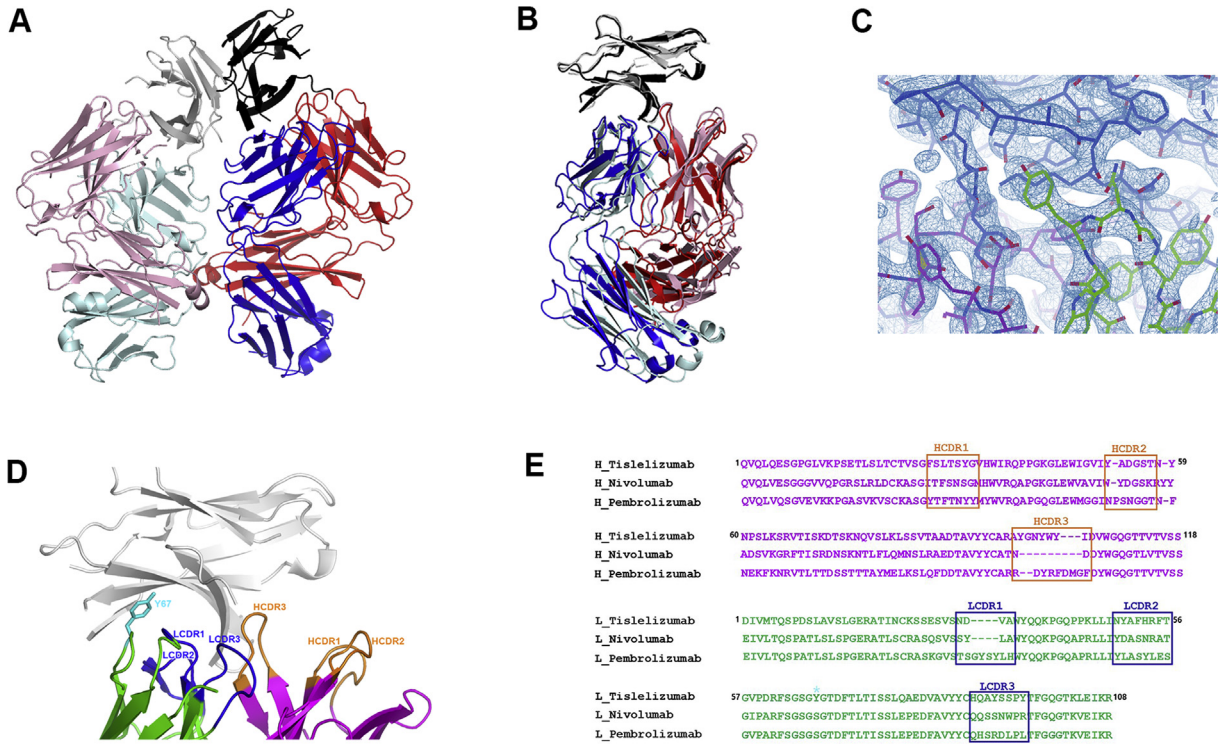

Fig. 1. Crystal structure of the PD-1/tislelizumab complex. (A) Two copies of the PD-1/tislelizumab complex in an asymmetric unit. PD-1 is colored black and gray. The heavy chain is colored red and pink, and the light chain blue and cyan. (B) Superposition of the PD-1 protein from the two copies in an asymmetric unit. (C) The 2fo-fc map (1.2 σ contour level) at the interface between PD-1 (blue) and tislelizumab (heavy chain: purple, light chain: green) calculated at 3.32 Å resolution. (D) The complementarity determining regions (CDRs) in the PD-1/tislelizumab complex structure. Y67 within the framework region of the tislelizumab light chain is colored cyan. (E) The amino acid sequences of the variable regions of the antibody drugs targeting PD-1. The residue numbers refer to those in tislelizumab. (For interpretation of the references to color in this figure legend, the reader is referred to the Web version of this article.)

between PD-1 and PD-L1 involves the front β-sheet faces of both immune checkpoint proteins, with additional contributions of the FG loop of PD-1. The epitope of tislelizumab is formed on the front β-sheet face of PD-1, which makes main interactions with PD-L1. In total, 12 residues of PD-1 are involved in the binding to tislelizumab with five hydrogen bonds and extensive van der Waals interactions

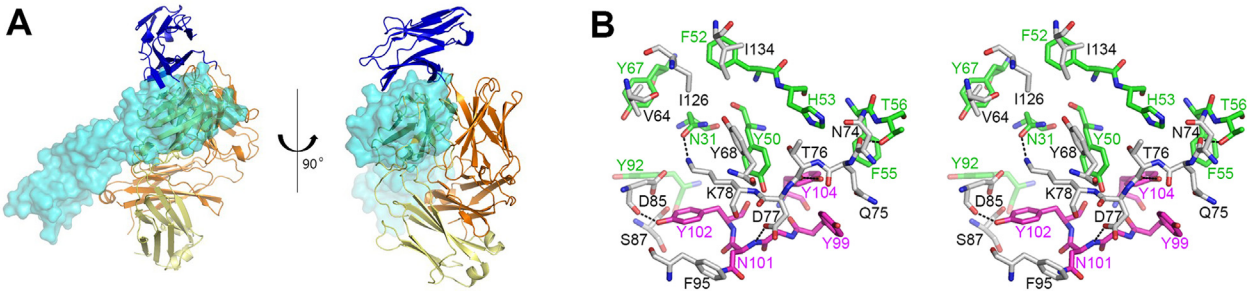

Fig. 2. Interaction of tislelizumab with PD-1. (A) Superposition of the tislelizumab/PD-1 complex structure with PD-1/PD-L1 complex structure (PDB code 3BIK) showing the competitive binding of tislelizumab and PD-L1 to PD-1. The structure of PD-1 (blue) in complex with tislelizumab is displayed as the ribbon model. The tislelizumab heavy and light chains are colored orange and yellow, respectively. The PD-L1 (cyan) in the PD-1/PD-L1 complex is displayed as the surface model. (B) Stereoscopic view of the detailed interactions in the interface between PD-1 and tislelizumab. The carbon atoms from PD-1 and the heavy and light chains of tislelizumab are colored white, purple, and green, respectively. Hydrogen bonds are indicated with dashed lines. (For interpretation of the references to color in this figure legend, the reader is referred to the Web version of this article.)

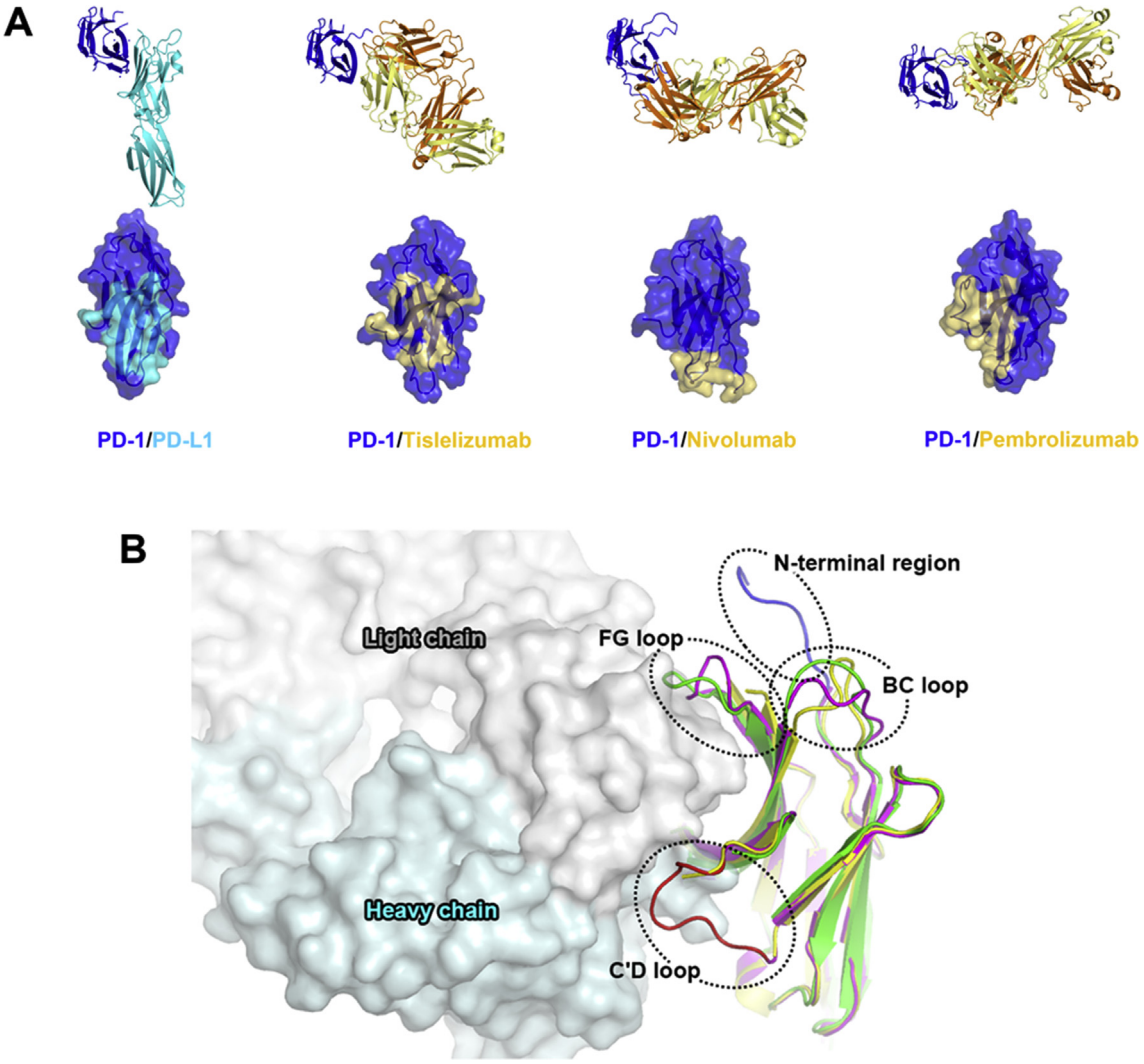

Fig. 3. Comparative binding of the monoclonal antibodies against PD-1. (A) Structures of PD-1 (blue) in complex with PD-L1 (cyan) or anti-PD-1 antibodies are displayed as the ribbon models (top). The antibody heavy and light chains are colored orange and yellow, respectively. The PD-L1 binding site (cyan) and the epitopes (yellow) of anti-PD-1 antibodies on PD-1 are displayed as the surface models (bottom). The structures of PD-1 are displayed in the same orientation. (**B**). Superposition of the PD-1 structures extracted from the complex structures of PD-1/tislelizumab (yellow), PD-1/pembrolizumab (purple, PDB code 5GGS), and PD-1/nivolumab (green, PDB code 5GGR) shows the variable conformations within the flexible loops of PD-1 induced by the binding of the antibody drugs. Tislelizumab in the complex structure of PD-1/tislelizumab is displayed as the surface model. The N-terminal region of PD-1 in the complex structure of PD-1/nivolumab is colored blue, and the C'D loop in PD-1/pembrolizumab is colored red. (For interpretation of the references to color in this figure legend, the reader is referred to the Web version of this article.)

(Fig. 2B). Although water molecules could mediate hydrogen bonds within the binding interface of the PD-1/tislelizumab complex, these cannot be included in the structure on account of the relatively low resolution of 3.32 Å. The side chains of $_{PD\text{-}1}$D77 and $_{PD\text{-}1}$K78 make hydrogen bonds with the backbone amide group of $_{heavy}$N101 and the side chain of $_{light}$N31, respectively. And the backbone carbonyl groups of $_{PD\text{-}1}$N74, $_{PD\text{-}1}$T76, and $_{PD\text{-}1}$D85 make hydrogen bonds with the side chains of $_{light}$T56, $_{heavy}$Y104, and $_{heavy}$Y102. The side chains of $_{PD\text{-}1}$Y68, $_{PD\text{-}1}$N74, $_{PD\text{-}1}$Q75, $_{PD\text{-}1}$T76, $_{PD\text{-}1}$D85, $_{PD\text{-}1}$S87, $_{PD\text{-}1}$F95, and $_{PD\text{-}1}$I134 on the front β-sheet face of PD-1 form van der Waals interactions with the residues within the CDRs of tislelizumab, including $_{light}$Y50, $_{light}$F52, $_{light}$H53, $_{light}$F55, $_{light}$T56, $_{light}$Y92, $_{heavy}$Y99, $_{heavy}$N101, $_{heavy}$Y102, and $_{heavy}$Y104. Interestingly, $_{light}$Y67, a residue within the framework region of the tislelizumab light chain, also contributes to the interaction with PD-1 by van der Waals contacts with $_{PD\text{-}1}$V64 and $_{PD\text{-}1}$I126 (Fig. 1D). The binding affinity (K_d) of tislelizumab to PD-1 was determined as 130 pM by surface plasmon resonance (SPR), whereas the K_d value of the PD-1/PD-L1 interaction was analyzed as 8.2 μM by SPR [25,26]. Taken together, all these interactions contribute to the high affinity of tislelizumab to PD-1, and these findings suggest that the binding of tislelizumab to PD-1 would abrogate the binding of PD-L1 with its much higher affinity to PD-1.

3.3. Comparison of the binding interactions of anti-PD-1 antibodies

The previously reported PD-1 complex structures of the US FDA-approved antibody drugs, nivolumab and pembrolizumab, enabled us to investigate the binding characteristics of these antibody drugs [14,17,18]. A comparative analysis of the PD-1 interactions with its ligand PD-L1 and the antibody drugs, including nivolumab, pembrolizumab, and tislelizumab, can provide not only a better understanding of the molecular mechanism of an antibody-based blockade of PD-1 but also an insight into the rational design of improved therapeutic antibodies targeting PD-1. The PD-1 structures extracted from the complex structures with PD-L1, nivolumab, and pembrolizumab were superimposed with that from the tislelizumab/PD-1 complex. The antibody drugs bind to PD-1 from various directions and on different binding sites (Fig. 3A). The interactions of tislelizumab are made by the front β-sheet face, while nivolumab and pembrolizumab mainly bind to the flexible loops of PD-1. As the interface between PD-1 and PD-L1 depends mostly on the residues of the front β-sheet of both proteins, the epitope of tislelizumab is very similar to the binding site of PD-L1 on the surface of PD-1. Interestingly, the interaction of tislelizumab does not involve the flexible loops of PD-1, unlike nivolumab and pembrolizumab (Fig. 3B). The binding of nivolumab mainly depends on the interaction with the N-terminal region of PD-1, while pembrolizumab primarily binds to the flexible C'D loop. Besides, the binding of nivolumab and pembrolizumab both induce structural changes in the flexible BC and FG loops of PD-1 for additional interaction with them [14]. However, none of the loop regions in PD-1 are involved in the interaction with tislelizumab. The C'D loop, N-terminal region, and FG loop are invisible in the structure of the tislelizumab/PD-1 complex, implying the lack of the interaction between these loop regions and tislelizumab. The BC loop is also located on the opposite side of the binding interface between PD-1 and tislelizumab. These findings demonstrate that antibody drugs against PD-1 adopt distinct binding modes to block the interaction between PD-1 and PD-L1.

4. Discussion

Antibody-based blockade of the PD-1/PD-L1 interaction has been significant therapy in immuno-oncology since the approval of the monoclonal antibodies against PD-1 or PD-L1. The antigenic epitope on a target protein is an essential characteristic of an antibody drug as different epitopes can bring about different therapeutic efficacy. Despite the common mechanism of the existing anti-PD-1 antibodies, the blockade of the interaction between PD-1 and PD-L1, these antibodies elicit various epitopes on the surface of PD-1 with distinct interactions. Structural studies to investigate specific epitopes and binding characteristics of therapeutic antibodies may facilitate the discovery of a better antibody with improved therapeutic efficacy. In the present study, the structural analysis revealed that tislelizumab mainly binds to the front β-sheet face comprising the CC'FG strands within PD-1, which is also the primary interface for PD-L1 binding, and the flexible loops of PD-1 are not involved in the antibody interaction. This binding mode of tislelizumab differs from that of nivolumab or pembrolizumab, which exhibits loop-dominated binding characteristics. The close overlap of the tislelizumab epitope with the PD-L1 binding site on the surface of PD-1 implies that the mechanism by which tislelizumab blocks the interaction between PD-1 and PD-L1 is by outcompeting PD-L1 for binding to PD-1 with its much higher affinity.

Author contributions

S.H.L., H.T.L., and H.L. performed sample preparation and crystallization. Y.K. and U.B.P performed data collection. S.H.L., H.T.L., and H.L. determined the structure. Y–S.H. designed the study and mainly wrote the manuscript with S.H.L., H.T.L., and H.L.

Data availability

Coordinates and structure factors have been deposited in the Protein Data Bank (http://www.rcsb.org), under the accession number 7BXA.

Declaration of competing interest

The authors declare no competing interests.

Acknowledgements

We are grateful to the staff of beamline 5C at Pohang Accelerator Laboratory for help with the X-ray diffraction experiments. This paper was supported by Konkuk University in 2017.

References

[1] Y. Ishida, Y. Agata, K. Shibahara, T. Honjo, Induced expression of PD-1, a novel member of the immunoglobulin gene superfamily, upon programmed cell death, EMBO J. 11 (1992) 3887–3895.
[2] G.J. Freeman, A.J. Long, Y. Iwai, K. Bourque, T. Chernova, H. Nishimura, L.J. Fitz, N. Malenkovich, T. Okazaki, M.C. Byrne, H.F. Horton, L. Fouser, L. Carter, V. Ling, M.R. Bowman, B.M. Carreno, M. Collins, C.R. Wood, T. Honjo, Engagement of the Pd-1 immunoinhibitory receptor by a novel B7 family member leads to negative regulation of lymphocyte activation, J. Exp. Med. 192 (2000) 1027–1034.
[3] Y. Latchman, C.R. Wood, T. Chernova, D. Chaudhary, M. Borde, I. Chernova, Y. Iwai, A.J. Long, J.A. Brown, R. Nunes, E.A. Greenfield, K. Bourque, V.A. Boussiotis, L.L. Carter, B.M. Carreno, N. Malenkovich, H. Nishimura, T. Okazaki, T. Honjo, A.H. Sharpe, G.J. Freeman, PD-L2 is a second ligand for PD-1 and inhibits T cell activation, Nat. Immunol. 2 (2001) 261–268.
[4] T.J. Curiel, S. Wei, H. Dong, X. Alvarez, P. Cheng, P. Mottram, R. Krzysiek, K.L. Knutson, B. Daniel, M.C. Zimmermann, O. David, M. Burow, A. Gordon, N. Dhurandhar, L. Myers, R. Berggren, A. Hemminki, R.D. Alvarez, D. Emilie, D.T. Curiel, L. Chen, W. Zou, Blockade of B7-H1 improves myeloid dendritic cell–mediated antitumor immunity, Nat. Med. 9 (2003) 562–567.
[5] F. Hirano, K. Kaneko, H. Tamura, H. Dong, S. Wang, M. Ichikawa, C. Rietz, D.B. Flies, J.S. Lau, G. Zhu, K. Tamada, L. Chen, Blockade of B7-H1 and PD-1 by monoclonal antibodies potentiates cancer therapeutic immunity, Canc. Res. 65 (2005) 1089–1096.

[6] W. Zou, J.D. Wolchok, L. Chen, PD-L1 (B7-H1) and PD-1 pathway blockade for cancer therapy: mechanisms, response biomarkers, and combinations, Sci. Transl. Med. 8 (2016), 328rv4-328rv4.
[7] L. Khoja, M.O. Butler, S.P. Kang, S. Ebbinghaus, A.M. Joshua, Pembrolizumab, J. Immunother, Cancer 3 (2015) 36.
[8] S.L. Topalian, F.S. Hodi, J.R. Brahmer, S.N. Gettinger, D.C. Smith, D.F. McDermott, J.D. Powderly, R.D. Carvajal, J.A. Sosman, M.B. Atkins, P.D. Leming, D.R. Spigel, S.J. Antonia, L. Horn, C.G. Drake, D.M. Pardoll, L. Chen, W.H. Sharfman, R.A. Anders, J.M. Taube, T.L. McMiller, H. Xu, A.J. Korman, M. Jure-Kunkel, S. Agrawal, D. McDonald, G.D. Kollia, A. Gupta, J.M. Wigginton, M. Sznol, Safety, activity, and immune correlates of anti–PD-1 antibody in cancer, N. Engl. J. Med. 366 (2012) 2443–2454.
[9] S.L. Topalian, M. Sznol, D.F. McDermott, H.M. Kluger, R.D. Carvajal, W.H. Sharfman, J.R. Brahmer, D.P. Lawrence, M.B. Atkins, J.D. Powderly, P.D. Leming, E.J. Lipson, I. Puzanov, D.C. Smith, J.M. Taube, J.M. Wigginton, G.D. Kollia, A. Gupta, D.M. Pardoll, J.A. Sosman, F.S. Hodi, Survival, durable tumor remission, and long-term safety in patients with advanced melanoma receiving nivolumab, J. Clin. Oncol. 32 (2014) 1020–1030.
[10] E.B. Garon, N.A. Rizvi, R. Hui, N. Leighl, A.S. Balmanoukian, J.P. Eder, A. Patnaik, C. Aggarwal, M. Gubens, L. Horn, E. Carcereny, M.-J. Ahn, E. Felip, J.-S. Lee, M.D. Hellmann, O. Hamid, J.W. Goldman, J.-C. Soria, M. Dolled-Filhart, R.Z. Rutledge, J. Zhang, J.K. Lunceford, R. Rangwala, G.M. Lubiniecki, C. Roach, K. Emancipator, L. Gandhi, Pembrolizumab for the treatment of non–small-cell lung cancer, N. Engl. J. Med. 372 (2015) 2018–2028.
[11] A. Markham, S. Duggan, Cemiplimab: first global approval, Drugs 78 (2018) 1841–1846.
[12] A. Lee, S.J. Keam, Tislelizumab: first approval, Drugs 80 (2020) 617–624.
[13] T. Zhang, X. Song, L. Xu, J. Ma, Y. Zhang, W. Gong, Y. Zhang, X. Zhou, Z. Wang, Y. Wang, Y. Shi, H. Bai, N. Liu, X. Yang, X. Cui, Y. Cao, Q. Liu, J. Song, Y. Li, Z. Tang, M. Guo, L. Wang, K. Li, The binding of an anti-PD-1 antibody to FcγRI has a profound impact on its biological functions, Cancer Immunol. Immunother. 67 (2018) 1079–1090.
[14] J.Y. Lee, H.T. Lee, W. Shin, J. Chae, J. Choi, S.H. Kim, H. Lim, T. Won Heo, K.Y. Park, Y.J. Lee, S.E. Ryu, J.Y. Son, J.U. Lee, Y.-S. Heo, Structural basis of checkpoint blockade by monoclonal antibodies in cancer immunotherapy, Nat. Commun. 7 (2016) 13354.
[15] H.T. Lee, J.Y. Lee, H. Lim, S.H. Lee, Y.J. Moon, H.J. Pyo, S.E. Ryu, W. Shin, Y.-S. Heo, Molecular mechanism of PD-1/PD-L1 blockade via anti-PD-L1 antibodies atezolizumab and durvalumab, Sci. Rep. 7 (2017) 5532.
[16] H. Lee, S. Lee, Y.-S. Heo, Molecular interactions of antibody drugs targeting PD-1, PD-L1, and CTLA-4 in immuno-oncology, Molecules 24 (2019) 1190.
[17] Z. Na, S.P. Yeo, S.R. Bharath, M.W. Bowler, E. Balıkçı, C.-I. Wang, H. Song, Structural basis for blocking PD-1-mediated immune suppression by therapeutic antibody pembrolizumab, Cell Res. 27 (2017) 147–150.
[18] S. Tan, H. Zhang, Y. Chai, H. Song, Z. Tong, Q. Wang, J. Qi, G. Wong, X. Zhu, W.J. Liu, S. Gao, Z. Wang, Y. Shi, F. Yang, G.F. Gao, J. Yan, An unexpected N-terminal loop in PD-1 dominates binding by nivolumab, Nat. Commun. 8 (2017) 14369.
[19] Z. Otwinowski, W. Minor, Processing of X-ray diffraction data collected in oscillation mode, Methods Enzymol. 276 (1997) 307–326.
[20] A.J. McCoy, R.W. Grosse-Kunstleve, P.D. Adams, M.D. Winn, L.C. Storoni, R.J. Read, Phaser crystallographic software, J. Appl. Crystallogr. 40 (2007) 658–674.
[21] P. Emsley, B. Lohkamp, W.G. Scott, K. Cowtan, Features and development of Coot, Acta Crystallogr. Sect. D Biol. Crystallogr. 66 (2010) 486–501.
[22] P.D. Adams, P.V. Afonine, G. Bunkóczi, V.B. Chen, I.W. Davis, N. Echols, J.J. Headd, L.-W. Hung, G.J. Kapral, R.W. Grosse-Kunstleve, A.J. McCoy, N.W. Moriarty, R. Oeffner, R.J. Read, D.C. Richardson, J.S. Richardson, T.C. Terwilliger, P.H. Zwart, PHENIX : a comprehensive Python-based system for macromolecular structure solution, Acta Crystallogr. Sect. D Biol. Crystallogr. 66 (2010) 213–221.
[23] D.Y. -w. Lin, Y. Tanaka, M. Iwasaki, A.G. Gittis, H.-P. Su, B. Mikami, T. Okazaki, T. Honjo, N. Minato, D.N. Garboczi, The PD-1/PD-L1 complex resembles the antigen-binding Fv domains of antibodies and T cell receptors, Proc. Natl. Acad. Sci. Unit. States Am. 105 (2008) 3011–3016.
[24] K.M. Zak, R. Kitel, S. Przetocka, P. Golik, K. Guzik, B. Musielak, A. Dömling, G. Dubin, T.A. Holak, Structure of the complex of human programmed death 1, PD-1, and its ligand PD-L1, Structure 23 (2015) 2341–2348.
[25] X. Cheng, V. Veverka, A. Radhakrishnan, L.C. Waters, F.W. Muskett, S.H. Morgan, J. Huo, C. Yu, E.J. Evans, A.J. Leslie, M. Griffiths, C. Stubberfield, R. Griffin, A.J. Henry, A. Jansson, J.E. Ladbury, S. Ikemizu, M.D. Carr, S.J. Davis, Structure and interactions of the human programmed cell death 1 receptor, J. Biol. Chem. 288 (2013) 11771–11785.
[26] M.E. Brown, D. Bedinger, A. Lilov, P. Rathanaswami, M. Vásquez, S. Durand, I. Wallace-Moyer, L. Zhong, J.H. Nett, I. Burnina, I. Caffry, H. Lynaugh, M. Sinclair, T. Sun, J. Bukowski, Y. Xu, Y.N. Abdiche, Assessing the binding properties of the anti-PD-1 antibody landscape using label-free biosensors, PLoS One 15 (2020), e0229206.